Separation of Excitation Forces from Simulated Gas Turbine Casing Response Measurements

Author/Contributor:
Forbes, Gareth Llewellyn; Randall, Robert Bond

Publication details:
Proceedings of the 7th European Conference on Structural Dynamics
9780854328826 (ISBN)

Event details:
7th European Conference on Structural Dynamics
Southampton, United Kingdom

Publication Date:
2008

DOI:
https://doi.org/10.26190/unsworks/358

7th European Conference on Structural Dynamics
EURODYN 2008
7-9 July 2008 Southampton

SEPARATION OF EXCITATION FORCES FROM SIMULATED GAS TURBINE CASING RESPONSE MEASUREMENTS

Gareth L. Forbes[1], Robert B. Randall[1]

[1]School of Mechanical and Manufacturing Engineering
University of New South Wales
P.O. Box 6359, 1466 UNSW Sydney, Australia
E-mail: gareth.forbes@student.unsw.edu.au
b.randall@unsw.edu.au

Keywords: Gas turbines, forced response, casing vibrations, cyclostationarity

ABSTRACT

Condition monitoring of blades within gas turbines has been and will continue to be of importance in all areas of their use, for maintenance and reliability purposes. Non-intrusive measurement of blade condition is the ambition of most techniques for this endeavour, with a number of methods proposed, investigated and employed for such measurement, with the current dominant method using proximity probes to measure blade arrival time for subsequent processing. It is proposed, however, that the measurement of the casing vibration, due to the aerodynamic-structural interaction within a gas turbine, could provide a means of blade condition monitoring and modal parameter estimation, without requiring perforation of the casing. An analytical model of a gas turbine casing and simulated pressure signal associated with the rotating blades, individual blade vibrations and transfer of stator blade vibrations has been developed in order to understand the complex relationship between casing response and the most important excitation forces.

Due to the force interaction being through a fluid medium, a certain degree of randomness is introduced into the excitations, and the viability of this inherent randomness as a useful aid for separation of the contributing excitation forces from the system response is explored.

1. INTRODUCTION

Blades within gas turbines operate under high unsteady pressure forces and turbulent pressure fluctuations at temperatures often approaching the design limit for metallic crystalline structure degradation. It is therefore not surprising that both forced vibration and heat transfer efficiency of turbine blades are of major concern in design and operation, and as such have been subject to a considerable amount of research study. Reduction of the forced vibration of blades is an important design factor to limit the dynamic forces to which the blades are subjected during operation. Traditionally, this promoted the use of the Campbell diagram to try to arrange design operating conditions such that the blades are not excited at a blade natural frequency. Furthermore the modeling of blade forced structural motion has advanced to take into account effects of wake passing, blade tip vortices, with semi-empirical models, as well as structural and aerodynamic loadings on blades [1], with further extensions using computational methods to calculate blade mode shapes and pressure loadings to better estimate the structural and aerodynamic loadings [2]. Having the ability to measure the forced vibration of the bladed arrangement during design to verify predicted vibrations is therefore advantageous. Under operating conditions the introduction of a fault in a gas turbine blade will alter the blade vibration properties and as the blades are under forced vibration, measurement of the blade vibration can lead to determination of a blade’s condition.

This need to measure blade vibration in both design and in operation has led to the development of the current dominant method; blade tip timing (BTT) for blade vibration measurement in the aero-industry [3, 4]. Measurements are taken using radially mounted proximity probes which measure the blade arrival times at different points around the casing in order to deduce blade vibration information. BTT methods are currently able to satisfactorily measure asynchronous, non-integer multiples of shaft speed, blade vibrations such as rotating stall, flutter and compressor surge, however no one single method is able to fully characterise the vibration parameters of blades in service [5].

An alternative method has been proposed for non-intrusive measurement of blade vibrations by means of external accelerometer measurements on the casing of a gas turbine [6]. This recent work however only dealt with the deterministic periodic forced blade vibrations, as is customary with blade vibration modeling and non-intrusive blade vibration measurement methods [1, 2, 7]. This current trend to model only the periodic forced responses within gas turbines in blade vibration models is thought to be driven by the fact that these periodic forces are usually the most destructive forces within an engine, which can cause large deflections and blade failure. It is however well understood that the operating conditions inside a gas turbine are highly turbulent, due to a wide variety of influences including; but not limited to, ingested turbulence, turbulent boundary layer flow, wake interaction, reversed flow and tip vortex flow. Each of these turbulent mechanisms have been investigated by numerous authors; (see for example [8-10]), however the motivation for understanding the turbulent flow phenomena has mainly been for the heat transfer efficiency and the aerodynamic efficiency of the blades through the boundary layer transition or separation [11, 12]. It has however been seen in a centrifugal compressor with no periodic pressure fluctuations, that the dominant excitation can be from broadband turbulent flow [13].

Without turbulence effects, the flow and pressure fluctuations would be purely deterministic and periodic, yet when the flow becomes turbulent these periodic pressure fluctuations become modulated by a random component. This is conventionally dealt with by adding a stationary random excitation component to the periodic forcing term, however it has been shown that a random amplitude modulated periodic signal is in fact cyclostationary, and displays periodicity in any second order statistic of the signal such as the variance, or autocorrelation function. [14]. The two-dimensional Fourier transform of the autocorrelation function is called the spectral correlation, and for second order cyclostationary signals is discrete in “cyclic frequency” α (Fourier transform with respect to normal time t exhibiting periodicity) while continuous in normal frequency f (Fourier transform with respect to time lag τ). This periodicity can then be exploited in separating differing signal types, viz; periodic, stationary random, and cyclostationary with different cyclic frequencies. This signal property has been successfully used in mechanical systems, for instance in the separation of bearing and gear faults [15], and is generally described as a signal processing tool for mechanical systems in [16]. The effects of cyclostationarity in the forced response of blades within turbo-machinery and simulation of the casing response under these operating conditions is explored in the subsequent sections.

2. FORCES ON CASING AND STATOR/ROTOR BLADES

The casing of a gas turbine, under test conditions, can be excited by two groups of forces [17], viz: (a) forces from the engine and running gear through casing/bearing attachments, (b) forces from the aerodynamic/structural interaction within the engine. The second group of forces, (b), can then be further broken down into its believed constituents; (i) interaction with the rotating pressure profile around each rotor/stator blade, (ii) propagation of acoustic waves inside the casing, (iii) pressure fluctuations due to turbulent and impulsive flows. The casing response due the steady state forces, (i), have been studied in [6]. As stated earlier, all known general blade forced response modelling and BTT techniques for measurement of blade response have only focused on the steady state response conditions. The current modelling takes into account the forces due to random turbulent flows, (iii), and in fact uses the inherent characteristics of these signal types to aid in the separation of the excitation forces.

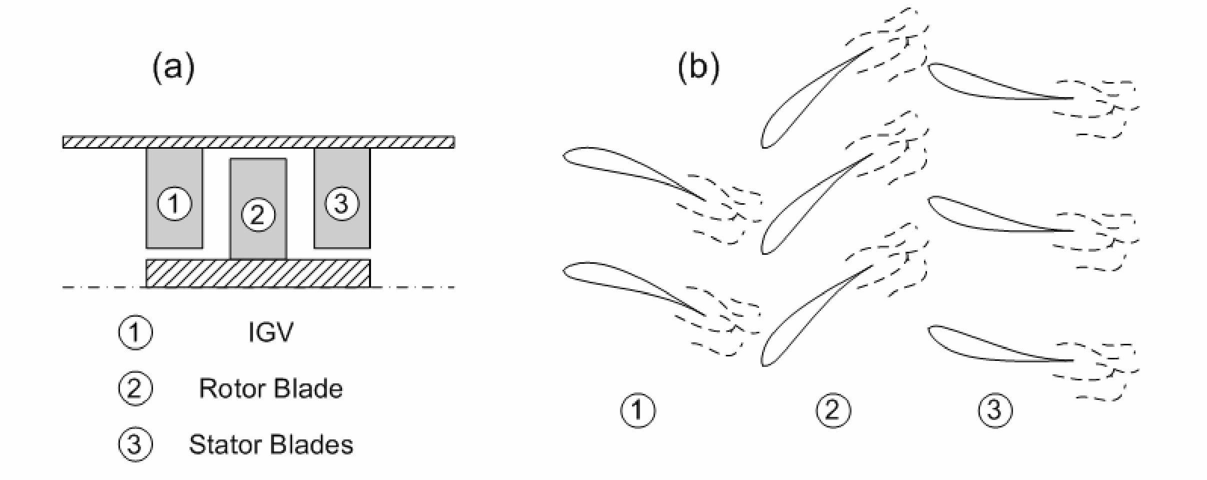

Figure 1 longitudinal section of 1.5 stage turbine (a), wake interaction between blade rows (b)

The current model is of a 1.5 stage turbine, with a row of 5 inlet guide vanes, IGV's, followed by a row of 6 rotor blades, with a final row of 5 stator blades. The IGV's and stator blades are also not "clocked", i.e. they are aligned axially. A longitudinal section of the simulated blade rows is shown in Figure 1(a), a transverse sectional view is seen in Figure 2.

In order to understand how the casing responds under the influence of the simulated operating conditions, we first discuss how the pressure profiles around each blade cause the casing to undergo forced vibration. In Figure 2, the first harmonic of the pressure field around the rotor blades, which rotates at the input shaft speed Ω, is displayed. It is clear that as this pressure profile rotates with shaft speed; there will be a fluctuating pressure on the inner surface of the casing. An equivalent static pressure field also exists around the stator blades. As a rotor blade goes past a stator blade, the pressure potential fields would interact with each other and provide a force on each. Along with the pressure potential around the blades, a more impulsive pressure fluctuation on the blades is introduced from the wakes behind leading blade rows which interact with downstream blade rows, as can be seen in Figure 1(b). Unlike the pressure potential effects, the wakes from upstream blades only affect downstream blades, whereas the pressure potential effects can affect both up- and downstream blade rows. The combination of the passing blade potentials and wake forces, often referred to as the pressure unsteadiness, therefore describe the total steady state force loadings on both the stator and rotor blades. It can now be seen that if all the blades undergo no deflection the response of the casing would be defined by its forced vibration under the effect of the rotating pressure profile around the rotor blades, and the forces transmitted through the stator blades, which in the limit would produce a local moment on the inside surface of the casing. This assumption of the stator blades remaining stationary will be maintained throughout the analysis, this being justified partly due to the fact that few stator blade vibration problems in turbo-machinery have been reported [18]. Stator blade vibration could however be included in more detailed models.

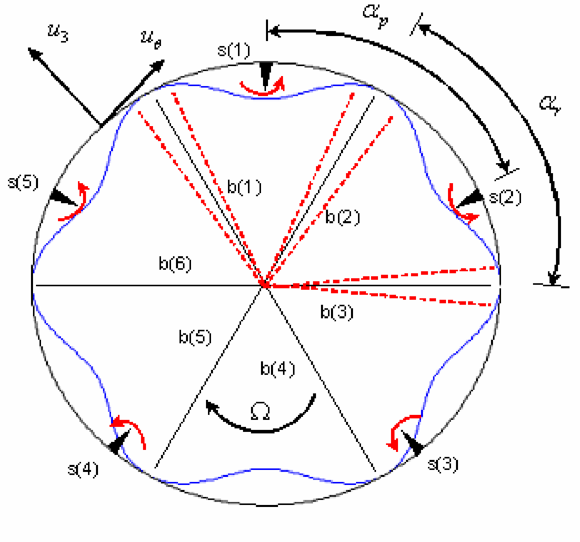

Figure 2 transverse sectional view of 1.5 stage turbine, s(1)-s(5) stator blade locations, b(1)-b(6) rotor blade locations

Now if the rotor blades are free to vibrate during the gas turbine operating cycle, the pressure around the rotor blades would vary in phase due to the blades' motion. Allowing each blade to vibrate individually, the rotating pressure field around each blade that acts on the casing surface, and the associated pressure profile around the blade following its motion, may be expressed mathematically as follows.

$$P_n = P.e^{jb\left[\theta - \Omega t - x(t)_r\right]}.\left[H\left(\theta - \Omega t - \alpha_r + \frac{\pi}{b}\right) - H\left(\theta - \Omega t - \alpha_r - \frac{\pi}{b}\right)\right] \qquad \textbf{(1)}$$

where H is the Heaviside function and $x(t)_r$ motion of the 'r^{th}' blade.

The forces on both the rotor and stator blades, downstream of a blade row, have been shown to have, in general, a damped impulse shape [10] (obviously this varies widely and is dependent on the specific turbine). The forces acting on the blade are therefore modelled as a raised cosine with a period of half the blade pass forcing frequency, as illustrated in Figure 3. The Fourier series expansion of this force on the 'r^{th}' blade can be expressed as:

$$f(t)_{r1} = F_0\left\{\sum_{i=0}^{\infty} A_i \cos\left[i\left(\omega_{spf} t + \gamma_r\right)\right]\right\} \qquad \textbf{(2)}$$

$$\gamma_r = \frac{2\pi(r-1)}{b} - \text{round}\left(\frac{s(r-1)}{b}\right)\frac{2\pi}{s} \qquad \textbf{(3)}$$

where A_i are the Fourier coefficients and ω_{spf} is the stator passing frequency.

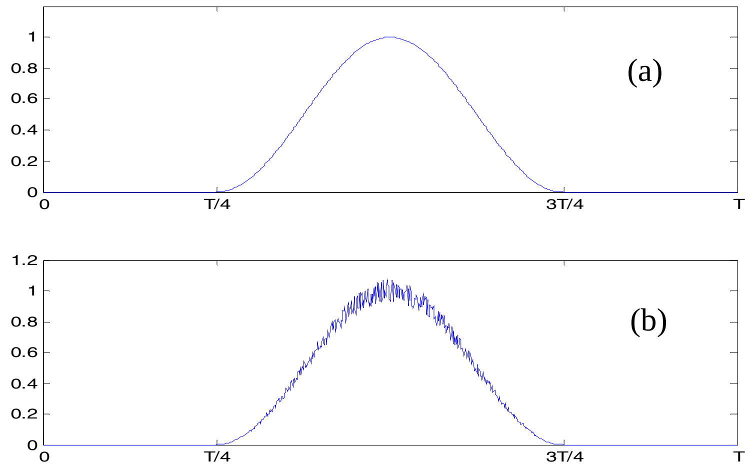

Figure 3 blade forcing function, purely deterministic (a), with random fluctuations (b)

Turbo-machinery flow conditions however are inherently turbulent, as stated earlier, with background turbulence intensity levels often reported to be approx. 3-4%, and turbulence within the wake region often 5 times greater than the background turbulence [8, 11, 19]. It is also noted that the frequency content of turbulence within a gas turbine will be somewhat band-limited, however in the context of this work the turbulence was assumed to be completely broadband. As the turbulence affects the magnitude of the blade pressure profile and pressure due to wake forces, this would then give a random amplitude modulation of the force on the blades, so the force including the turbulent fluctuations on the 'r^{th}' blade can now be expressed as (it is to be noted in this study only the effect of random fluctuations on the blade motion were considered, and not the random fluctuations on absolute magnitude of the pressure on stator blades and casing surface):

$$f(t)_{r2} = F_0\left(b(t)+1\right)\left\{\sum_{i=0}^{\infty} A_i \cos\left[i\left(\omega_{spf}t+\gamma_r\right)\right]\right\} \quad \textbf{(4)}$$

where $b(t)$ is a uniformly distributed random variable with zero mean and deviation of $\pm 7.5\%$.

Lastly the force transmitted to the casing through the stator blades, with their dynamic motion neglected, can be applied as a discrete moment at the location of the stator blade attachment, with the same form as the loading on the rotor blades as given in equation (4), however the phase will now be dependent on the rotor blades' motion such that the resulting moment for the 'p^{th}' stator blade can be expressed as:

$$T_p = M_0\left\{\sum_{r=1}^{b}\sum_{j=0}^{\infty} A_j \cos\left[j\left(\Omega t - x(t)_r + \alpha_r - \alpha_p\right)\right]\right\}\delta\left(\theta-\alpha_p\right)\left(\frac{1}{R}\right) \quad \textbf{(5)}$$

The turbulence effects can be seen in the above equations to influence the forces causing the rotor blade motion; however, they also affect the direct pressures acting on the casing through the phase modulation of the rotating pressure field and moment loadings on the casing from the stator blades.

3. BLADE FORCED VIBRATION SOLUTION

The force acting on the rotor and stator blades has now been defined in equation (4), with terms for both the pressure unsteadiness, the deterministic component; and the turbulence, the random component. The blade is assumed to act as a simple oscillator, i.e. a single degree of freedom spring-mass-damper system, this has been stated to be an adequate model of the blade's response if only one natural frequency is near the excitation frequencies [7], it has also been stated that at most a two degree of freedom system would adequately model the blades' forced vibration at any given operating condition (bending and twisting). All blades have been given an arbitrary natural frequency of 500Hz, with no coupling between blades or mistuning effects, with light damping of $\zeta = 0.005$, and the blades' maximum deflection is limited to $\pi / 2b$, or one quarter of the blade spacing, at resonance.

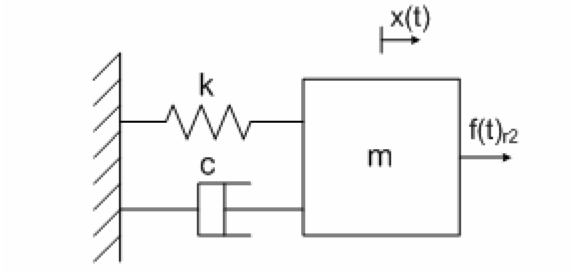

Figure 4 single degree of freedom blade model

The solution for the forced response of the above SDOF system, under a deterministic forcing function is easily shown to be:

$$x(t)_{rd} = \sum_{i=0}^{\infty} X_{ir} \cos\left[i\left(\omega_{spf} t - \phi_{ir} + \gamma_r \right) \right] \quad \textbf{(6)}$$

where X_{ib} and ϕ_{ib} are the non-dimensional amplitude and phase for the 'r^{th}' rotor blade, and can be found in any general vibration text such as [20].

The blades' motion for the deterministic part of $f(t)_{r2}$ is now fully defined. However, if we now look back at the random component of equation (4), we see that we have an amplitude modulated random signal, which is a classic type of cyclostationary signal [14]. It is however purely stochastic which makes it relatively straightforward to solve for the blades' response to this signal.

The normal procedure to solve for the response of a linear time invariant, LTIV, filter to a random input is to express the Power Spectral Density, PSD, as:

$$S_y(\omega) = H(\omega) H^*(\omega) S_x(\omega) \quad \textbf{(7)}$$

$$S_x(\omega) = \lim_{W \to \infty} \frac{1}{W} E\left\{ X_W(\omega) X_W^*(\omega) \right\} \quad \textbf{(8)}$$

where * is the conjugate operator.

Now the response of the blade can be seen to be defined for the entire forcing function, equation (4).

4. CASING RESPONSE SOLUTION

The response of the blade under the specific loading conditions was shown in the previous section, now the casing response under the influence of the forces given in equations (1) and (5) can be undertaken. The casing was modelled as an ideal circular ring, with the geometric and material properties as given in Table 1. The equations of motion are then solved for the circular ring under the given forces to provide a complete analytical closed form simulated solution.

Table 1 Geometric and material properties of ring

Density	$\rho = 7.85 \times 10^{-9} Ns^2 / mm^4$
Young's Modulus	$E = 20.6 \times 10^4 N / mm^2$
Mean Radius	$R = 100mm$
Radial Thickness	$h = 2mm$
Damping	$\zeta = 0.01$

4.1 RESPONSE DUE TO ROTATING PRESSURE FIELD

For both the deterministic and random blade vibrations the solution is undertaken by first solving the generalised force vector for the system. The generalised force vector is given as:

$$F_{nk} = \frac{1}{2\rho h N_{nk}} \int_{\theta} P_n .conj\left(U_{3k}\right) R d\theta \qquad \textbf{(9)}$$

The necessary mode shapes for an elastic ring under a moving load are given below [21], the solution is also only solved for $k = 1$, as the lowest natural frequency at $k = 2$, is an order of magnitude above blade pass frequency, BPF.

$$U_3 = e^{jn(\theta - \alpha_r)} \qquad \textbf{(10)}$$

It is also shown that:

$$N_n = \pi\left(1 + C_n^2\right) R \qquad \textbf{(11)}$$

and approximated:

$$C_n \approx -1/n \qquad \textbf{(12)}$$

The generalised force vector can therefore be shown to be:

$$F_n = \frac{P.R.f\left(n\right)}{2\rho h N_n} .e^{-i\left[n\Omega t + b.x(t)_r\right]} \qquad \textbf{(13)}$$

$$f\left(n\right) = \begin{cases} \dfrac{2}{b-n}\sin\left(\dfrac{\left(b-n\right)\pi}{b}\right) & n \neq b \\ \dfrac{2\pi}{b} & n = b \end{cases} \qquad \textbf{(14)}$$

The solution for the periodic part of a blade's response, $x\left(t\right)_{rd}$, is given by:

$$u_{3d} = \mathrm{Re}\left[\sum_{i=0}^{\infty} \sum_{n=1}^{\infty} \sum_{v=-\infty}^{\infty} \sum_{r=1}^{b} a_{ni} e^{j\left(n\theta - n\Omega t - v\left(i\omega_{spf} t + \gamma_r + \varphi_{ir}\right) - \psi_{ni} - n\alpha_r\right)} \right] \quad \textbf{(15)}$$

$$a_{ni} = \frac{P.R.f(n).J_v(b.X_{ir})}{2\rho h N_n \sqrt{\left(n^2 \tilde{\omega}_n^2 - n^2\left(\Omega - vi\omega_{spf}/n\right)^2\right)^2 + 4\zeta^2 \tilde{\omega}_n^2 n^4 \left(\Omega - vi\omega_{spf}/n\right)^2}} \quad \textbf{(16)}$$

$$\psi_{ni} = \tan^{-1}\left(\frac{2\zeta\left(\frac{\Omega - vi\omega_{spf}/n}{\tilde{\omega}_n}\right)}{1 - \left(\frac{\Omega - vi\omega_{spf}/n}{\tilde{\omega}_n}\right)^2} \right) \quad \textbf{(17)}$$

where $\tilde{\omega}_n = \omega_n / n$.

The solution for the random component of the blade motion on the rotating pressure field is solved in the same manner for a stochastic process as for the blade random excitation given in equation (7).

4.2 RESPONSE DUE TO STATOR BLADE LOADINGS

The same methodology for the stator blade loadings will be used as for the rotating pressure field. With first solution of the generalised force vector, which can be shown for a moment load on an elastic ring to be given by [22].

$$F_n = \frac{1}{\rho h N_n} \int_{\theta} U_3 \left[\frac{\partial\left(T_p R\right)}{\partial \theta} \right] d\theta \quad \textbf{(18)}$$

where the mode shapes are now given as:

$$U_3 = \cos n\left(\theta - \phi_p\right) \quad \textbf{(19)}$$

The solution for the generalised force vector is now given as:

$$F_n = \frac{M_0 n}{\rho h N_n} \sum_{j=0}^{\infty} \left\{ A_j \cos\left[j\left(\omega_{bpf} t + \gamma_p - x(t)_r + \phi_j\right)\right]\right\} \quad \textbf{(20)}$$

$$\gamma_p = \mathrm{round}\left(\frac{\mathrm{b}(p-1)}{s}\right)\frac{2\pi}{b} - \frac{2\pi(p-1)}{s} \quad \textbf{(21)}$$

setting the condition that:

$$\phi_p = -\frac{\pi}{2n} + \alpha_p \quad \textbf{(22)}$$

The solution to the deterministic part of the blade vibration is given as:

$$u_{3d} = \sum_{j=0}^{\infty}\sum_{i=0}^{\infty}\sum_{n=0}^{\infty}\sum_{p=1}^{s}\sum_{\nu=-\infty}^{\infty} \frac{M_0 n J_\nu\left(X_{ir}\right) A_n}{\rho h N_n} \left\{ A_j \cos\left[j\left(\omega_{bpf} t + \gamma_p - \nu\left(i\omega_{spf} t + \phi_i\right) - \phi_n + \phi_j\right)\right]\right\} . \cos n\left(\theta - \phi_p\right)$$

(23)

$$A_n = \frac{1}{\omega_n^2 \sqrt{\left[1-\left(\omega/\omega_n\right)^2\right] + 4\zeta^2\left(\omega/\omega_n\right)^2}} \quad \textbf{(24)}$$

$$\phi_n = \tan^{-1}\left(\frac{2\zeta\left(\omega/\omega_n\right)}{1-\left(\omega/\omega_n\right)}\right) \quad \textbf{(25)}$$

The solution to the random part of the blade vibration is once again solved for in the same manner as outlined in preceding sections. It will however be shown here for clarity how the random forcing function on the rotor blades propagates through to a random force on the casing through the stator blade loadings and contains information on the blade vibrations themselves.

Substitution of the instantaneous stochastic blade vibrations into equation (20), gives the generalised force vector for loading on each stator blade.

$$F_{n,random} = \sum_{r=1}^{b}\sum_{j=0}^{\infty} \frac{M_0 n}{\rho h N_n} A_j \left\{ \cos\left[j\left(\Omega t + \alpha_r - \alpha_p\right)\right] . \cos\left(x_r\right) + \sin\left[j\left(\Omega t + \alpha_r - \alpha_p\right)\right] . \sin\left(x_r\right)\right\} \quad \textbf{(26)}$$

where x_{random} is the instantaneous time signal of the blade motion under the stochastic part of the forcing function. The PSD, of the casing vibration would therefore be comprised of the generalised force on each stator blade after it passes through the LTIV filter of the casing's structural transfer function. From equation (26), it can be seen that the random blade vibrations are multiplied by *'j'* multiples of Ω. This causes, not initially intuitively, the response for the blade structural response, with a peak at its natural frequency, to be present in the PSD at the multiples of shaft speed, Ω, $\pm$ blade natural frequency.

5. RESULTS

Results were obtained for the radial displacement of a circular ring under the loading conditions outlined earlier, with an input shaft speed, Ω, of 80 Hz. The analytical solution of the PSD is shown in Figure 5, the response form is seen to be made up of discrete peaks at multiples of shaft speed, with the dominant peak being at BPF, which is what was observed in [6]. Underlying the discrete peaks is the casing structural response as excited by the stochastic part of the blade forcing function. Separation of the periodic discrete contribution to the casing PSD is relatively straightforward with a range of techniques available, such as synchronous averaging. Once separated the deterministic components or the residual signal can be further utilised. It is in this instance the residual signal which is to be further examined, as is illustrated in Figure 6. The residual PSD can be seen to have multiple peaks not at the locations of structural resonance of the ring, these peaks are in-fact the forcing function, given in equation (4), filtered by the structural response of the blade. The peaks appear at multiples of shaft speed $\pm$ the blade natural frequency for the contribution given by both the stator blade loadings and rotating internal pressure field. Interestingly, for the rotating pressure load, the contribution at any integer multiple of shaft speed comes solely from the same integer numbered mode.

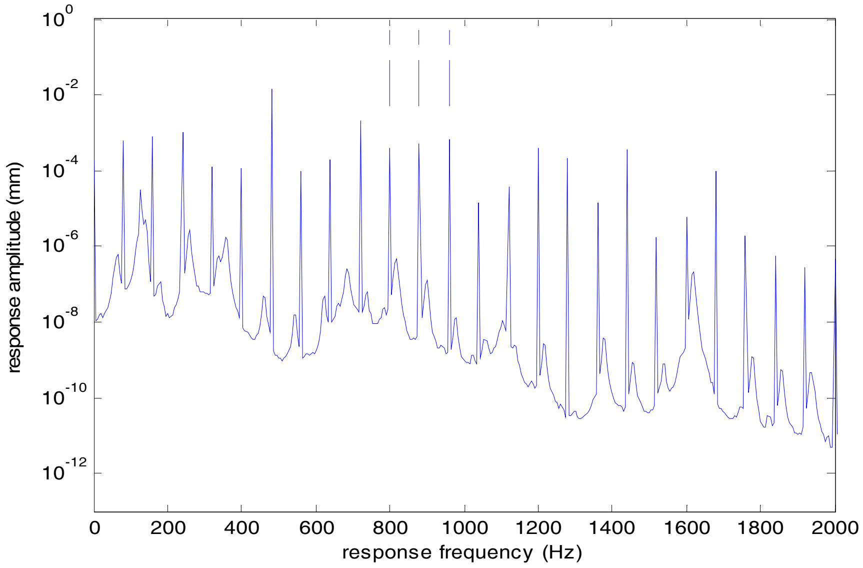

Figure 5 PSD of total casing response, vertical dashed lines at shaft speed spacing

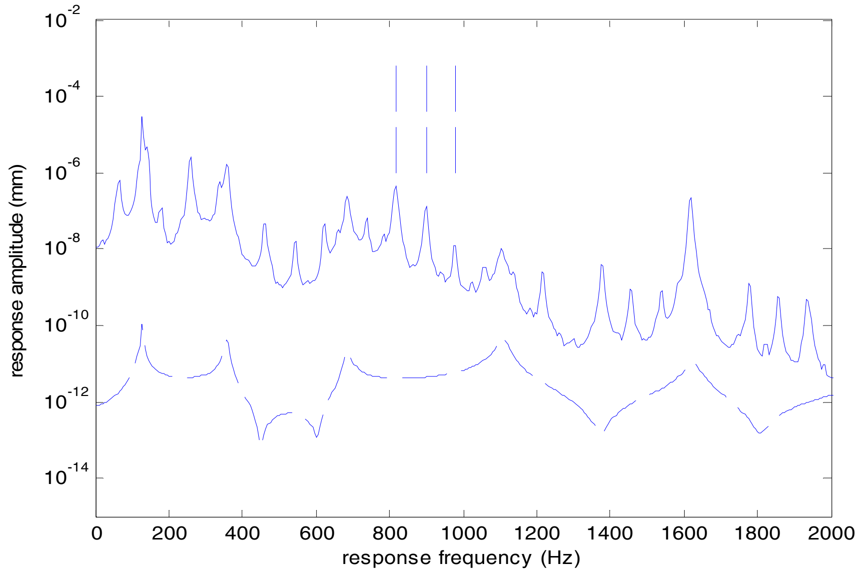

Figure 6 Residual PSD —— , structural transfer function ---- , vertical dashed lines at (4-6)$\times$shaft speed + blade natural frequency.

Although the PSD of the casing vibrations can be seen to show information pertaining to the rotor blade vibrations, if more than a single stage turbine was analysed the contribution from each stage would be masked by excitations from other stages. It is therefore advantageous that a single stage may be extracted from the overall measurements. This could be done by exploiting the cyclostationary properties that the stochastic forcing signal contains. Contributions to the casing vibration from the stator blades and rotating pressure field, from a given stage, can be seen to have cyclic frequencies of $i\omega_{spf} \pm j\Omega$ and $i\omega_{spf} \pm n\Omega$ respectively. Although contributions are not unique for each stage, as all stage frequencies are harmonics of shaft speed, the contribution at harmonics corresponding to the sums of multiples of a particular SPF and the down stream BPF are presumed to be dominant.

Shown in Figure 7 is the cyclic spectrum (spectral correlation for a particular cyclic frequency) at a cyclic frequency of twice the sum of BPF and SPF. The contribution at this cyclic frequency would be dominated by this engine stage, even if other engine stage contributions were also present, and this would aid in separating different blade stages. It is also noted that the peaks in the PSD given by the blade natural frequency have all shifted by an amount α, which causes the multiples of shaft speed minus blade natural frequency which wrap around zero frequency to be more prominent, as shown by the dotted lines in Figure 6. This is due to the fact that the cyclic spectrum is derived as follows:

$$S_y^{\alpha}(\omega) = H(\omega) H^*(\omega - \alpha) S_x^{\alpha}(\omega) \quad \textbf{(27)}$$

$$S_x^{\alpha} = \lim_{W \to \infty} \frac{1}{W} E\left\{ X_W(\omega) X^*(\omega - \alpha) \right\} \quad \textbf{(28)}$$

And highlights phenomena happening at cyclic frequency α.

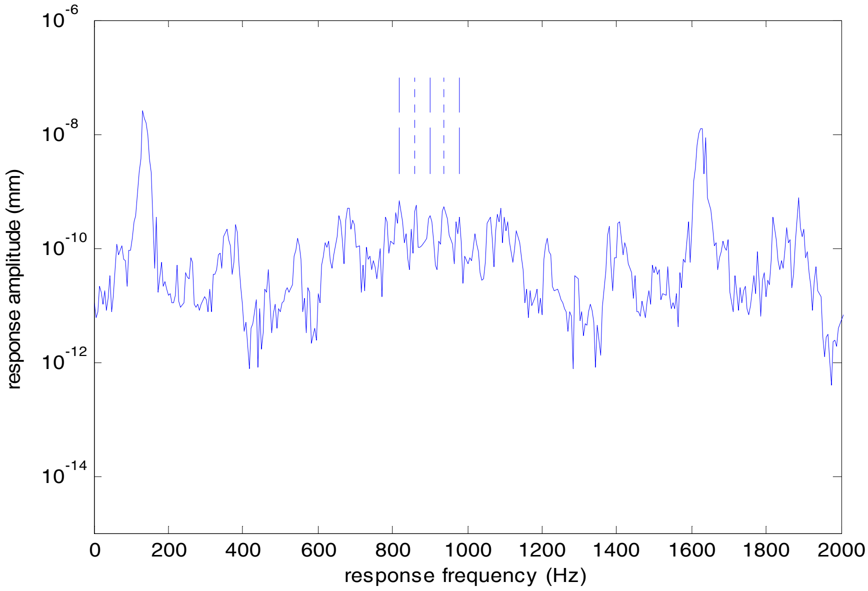

Figure 7 Cyclic spectrum at $\alpha = 2(BPF + SPF)$, vertical dashed lines at (4-6)$\times$shaft speed + blade natural frequency, vertical dotted lines at frequencies wrapped around zero.

6. CONCLUSIONS

The closed form analytical solution for a circular ring, under the simulated operating conditions for a gas turbine with both periodic and turbulent force components included, has been presented. Importantly, the random contribution to the excitation of the casing and the rotor blades has been shown to contain information of the blade vibration characteristics. The separation of the different force signal types was also shown, with periodic contributions removed and the potential ability to separate the contribution to the casing vibration for different stages by taking advantage of the signal’s inherent cyclostationary properties.

7. ACKNOWLEDGMENTS

Grateful acknowledgment is made for the financial assistance given by the Australian Defence Science and Technology Organisation, under the Centre of Expertise in Helicopter Structures and Diagnostics at UNSW.

8. REFERENCES

[1.] Majjigi, R.K. and P.R. Gliebe, *Development of rotor wake/vortex model*, in *NASA-CR-174849*. 1984, NASA contract NAS3-23681.

[2.] Chiang, H.-W.D. and R.E. Kielb, *Analysis system for blade forced response.* Journal of Turbomachinery, Transactions of the ASME, 1993. **115**(4): p. 762-770.

[3.] Zielinski, M. and G. Ziller, *Noncontact Blade Vibration Measurement System for Aero Engine Application.* American Institute of Aeronautics and Astronautics, 2005(ISABE).

[4.] Heath, S., *A New Technique for Identifying Synchronous Resonances Using Tip-Timing.* Journal of Engineering for Gas Turbines and Power, 2000. **122**(2): p. 219-225.

[5.] Heath, S., et al. *Turbomachinery blade tip measurement techniques*. in *Advanced Non-Intrusive Instrumentation for Propulsion Engines*. 1997. Brussels, Belgium.

[6.] Forbes, G.L. and R.B. Randall. *Simulated Gas Turbine Casing Response to Rotor Blade Pressure Excitation*. in *5th Australiasian Congress on Applied Mechanics*. 2007. Brisbane, Australia.

[7.] Dimitriadis, G., et al., *Blade-tip timing measurement of synchronous vibrations of rotating bladed assemblies.* Mechanical Systems and Signal Processing, 2002. **16**(4): p. 599-622.

[8.] Henderson, A.D., G.J. Walker, and J.D. Hughes, *The influence of turbulence on wake dispersion and blade row interaction in an axial compressor.* Journal of Turbomachinery, 2006. **128**(1): p. 150-157.

[9.] Kameier, F. and W. Neise, *Rotating blade flow instability as a source of noise in axial turbomachines.* Journal of Sound and Vibration, 1997. **203**(5): p. 833-853.

[10.] Mailach, R., L. Muller, and K. Vogeler, *Rotor-stator interactions in a four-stage low-speed axial compressor - Part II: Unsteady aerodynamic forces of rotor and stator blades.* Journal of Turbomachinery, 2004. **126**(4): p. 519-526.

[11.] Dullenkopf, K. and R.E. Mayle, *Effects of incident turbulence and moving wakes on laminar heat transfer in gas turbines.* Journal of Turbomachinery, Transactions of the ASME, 1994. **116**(1): p. 23-28.

[12.] Mailach, R. and K. Vogeler, *Aerodynamic blade row interactions in an axial compressor - Part I: Unsteady boundary layer development.* Journal of Turbomachinery, 2004. **126**(1): p. 35-44.

[13.] Haupt, U., M. Rautenberg, and A.N. Abdel-Hamid, *Blade Excitation by Broad-Band Pressure Fluctuations in a Centrifugal Compressor.* Journal of Turbomachinery, 1988. **110**(1): p. 129-137.

[14.] Gardner, W.A., *Cyclostationarity in communications and signal processing*. 1994, New York: IEEE Press. xiv, 504 p.

[15.] Antoni, J. and R.B. Randall, *Differential diagnosis of gear and bearing faults.* Journal of Vibration and Acoustics, Transactions of the ASME, 2002. **124**(2): p. 165-171.

[16.] Antoni, J., et al., *Cyclostationary modelling of rotating machine vibration signals.* Mechanical Systems and Signal Processing, 2004. **18**(6): p. 1285-1314.

[17.] Mathioudakis, K., E. Loukis, and K.D. Papailiou. *Casing vibration and gas turbine operating conditions*. 1989. Toronto, Ont, Can: Publ by American Soc of Mechanical Engineers (ASME), New York, NY, USA.

[18.] Cumpsty, N.A., *Compressor Aerodynamics*. 2004: Krieger Publishing Company.

[19.] Camp, T.R. and H.W. Shin, *Turbulence intensity and length scale measurements in multistage compressors.* Journal of Turbomachinery, Transactions of the ASME, 1995. **117**(1): p. 38-46.

[20.] Rao, S.S., *Mechanical vibrations*. 4th ed. 2004, Upper Saddle River, N.J.: Pearson Prentice Hall. xxvi, 1078 p.

[21.] Forbes, G.L. and R.B. Randall, *Resonance Phenomena of an Elastic Ring under a Moving Load.* Journal of Sound and Vibration, 2008. **Under Review**.

[22.] Soedel, W., *Vibrations of shells and plates*. 2nd ed. 1993, New York: Marcel Dekker. xix, 470 p.